ELSEVIER

Powder Technology 81 (1994) 125–137

POWDER TECHNOLOGY

Pressure drop prediction in low-velocity pneumatic conveying

B. Mi, P.W. Wypych *

Department of Mechanical Engineering, University of Woolongong, Northfields Avenue, Wollongong NSW 2522, Australia

Received 20 August 1993; in revised form 1 July 1994

Abstract

Low-velocity slug-flow pneumatic conveying is being applied to an increasing number of applications due to reasons of low power consumption and low product damage. In order to investigate improved design and scale-up procedures, several granular products are conveyed initially in a low-velocity pneumatic conveying test rig comprising various combinations of length and diameter (e.g. $L=52$, 96 m; $D=105$ mm). Based on these experimental investigations and a force balance of the moving slugs, a semi-empirical model is developed to predict the overall pipeline pressure drop in the horizontal slug-flow of cohesionless bulk solids. Model predictions compare well with additional experimental data obtained on 105 and 156 mm internal diameter horizontal pipelines. A method for determining the optimal operating point for low-velocity slug-flow is also presented.

Keywords: Pressure drop; Low-velocity pneumatic conveying

1. Introduction

The applications of low-velocity slug-flow pneumatic conveying have received increased attention in recent years due to features, such as low power consumption, product degradation and pipe wear. A general description of this mode of flow together with important design considerations has been presented by Wypych and Hauser [1].

Due to the complex nature of flow, only a few theoretical investigations have been carried out [2,3], and some of the factors affecting conveying performance have still not been solved completely. For example, Konrad and Harrison [2] applied the principles of powder mechanics and Ergun's equation to a moving slug which was assumed as a packed bed, and then developed a method for the theoretical calculation of the mean velocity of particles contained in the slug. However, the particle slug is actually an aerated bed in most cases and Ergun's equation is no longer applicable. Also, the transmission ratio of radial stress to axial stress was not able to be determined in earlier research investigations.

This paper applies the principles of powder mechanics to a moving slug to obtain a theoretical relationship for the pressure variation in the slug. A large-scale low-velocity test rig is also constructed and employed to investigate factors which are difficult to determine by theory (e.g. slug velocity, stress transmission coefficient, etc.). Based on these experimental results, a semi-empirical pressure drop model is developed and applied to the optimisation of system operation (based on minimum energy consumption).

2. Force balance and pressure gradient

Fig. 1 shows a particle slug element which is subjected to air pressure and stresses in a horizontal pipe. The notations in the Figure are as follows. p and dp are the air pressure and its increment in the x direction. The pressure forces acting on the two sides of the

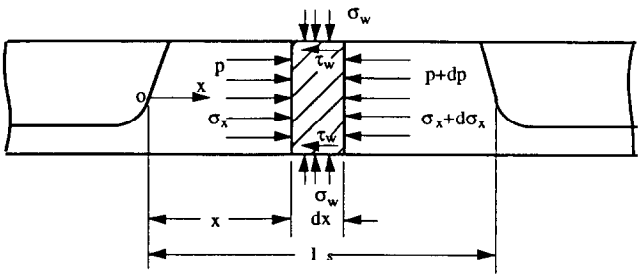

Fig. 1. Air pressure and stresses acting on a horizontal particle slug.

*Corresponding author.

SSDI 0032-5910(94)2875-O

element are pA and $(p+dp)A$, respectively, where cross-sectional area $A=\pi D^2/4$ and D = internal diameter of pipe. The external forces in the flow direction compress the particles inside the slug, resulting in σ_x and its increment $d\sigma_x$, as shown in Fig. 1. The corresponding forces acting on the element are $\sigma_x A$ and $(\sigma_x+d\sigma_x)A$.

Stress σ_w is the normal wall pressure acting perpendicularly to the pipe wall. It is believed that wall pressure is composed of two parts for horizontal slug flow, as shown in Fig. 2. σ_{sw} is a direct result of material weight. In Fig. 3, $\sigma_{sw}=(1+\cos\theta)\rho_b gR$. The radial compression stress σ_{rw} is caused by the pipe wall reacting against the axial compression stress σ_x. The ratio

$$\lambda=\sigma_r/\sigma_x \tag{1}$$

is called the force (stress) transmission coefficient. It is also known as the stress ratio of horizontal to vertical stress for the calculation of stresses in silos and hoppers [3]. For a slug moving in a pipe with rigid and parallel walls, Mi and Wypych [4] suggested from a theoretical analysis that

$$\lambda=\frac{\sigma_{rw}}{\sigma_x}=\frac{1-\sin\phi_s\cos(\omega-\phi_w)}{1+\sin\phi_s\cos(\omega-\phi_w)} \tag{2}$$

$$\sin\omega=\sin\phi_w/\sin\phi_s \tag{3}$$

where ϕ_s is defined as the internal static friction angle. Its value is less than the internal friction angle ϕ and is investigated further by experiment. ϕ_w is the wall friction angle. Note that the derivation of Eqs. (2) and (3) is presented in the Appendix.

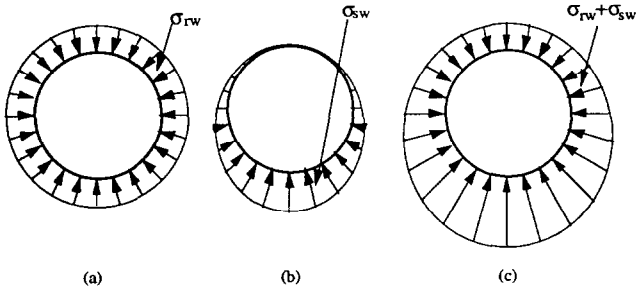

Fig. 2. (a) Inter-particle radial stress at the wall; (b) normal wall stress due to material weight; (c) wall pressure (i.e. total normal wall stress).

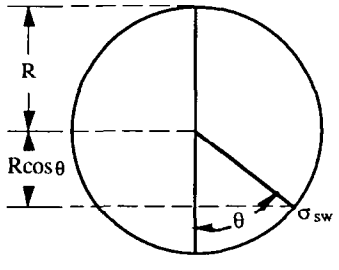

Fig. 3. Cross section of a slug.

τ_w is the shear stress at the wall. If the material obeys the Coulomb failure criterion, then $\tau_w=\mu_w\sigma_w+c_w$, where $\mu_w=\tan\phi_w$ and c_w is the particle cohesion at the wall. Note for cohesionless material, $c_w=0$. As this study is confined to free-flowing granular materials, $\tau_w=\mu_w[\sigma_{rw}+(1+\cos\theta)\rho_b gR]$. Thus the wall friction force is $2\int_0^{\pi}\tau_w R\,d\theta\,dx$ for a slug length of dx.

When a moving slug reaches steady state, there is an equilibrium between the driving force and resistant force. Assuming the axial stress and its radial transmission stress are functions of x only, the balance of the forces acting on the element of length dx results in

$$\frac{dp}{dx}+\frac{d\sigma_x}{dx}+\frac{\int_0^{2\pi}\tau_w R\,d\theta}{A}=0 \tag{4}$$

If the pressure gradient is assumed constant, then $dp/dx=-\Delta p/l_s$, where l_s is the length of a single slug. The solution to Eq. (4) is therefore

$$\sigma_x=c\exp\left(-\frac{2\mu_w\lambda}{R}x\right)+\left(-2\rho_b g\mu_w+\frac{\Delta p}{l_s}\right)\frac{D}{4\mu_w\lambda} \tag{5}$$

where c is an integration constant and can be determined by applying the following boundary conditions where the stresses on the front and back faces are σ_f and σ_b, respectively.

$\sigma_x=\sigma_f$, at $x=l_s$,

$\sigma_x=\sigma_b$, at $x=0$

Applying the above conditions, and assuming $l_s\gg D$, which is reasonable for a natural slug-flow system, an equation for pressure gradient of a single horizontal slug can be determined:

$$\frac{\Delta p}{l_s}=\frac{4\mu_w\lambda}{D}\sigma_f+2\rho_b g\mu_w \tag{6}$$

The stress σ_f in Eq. (6) is caused by the 'collection' of the particles from the stationary bed. An estimation of its value can be determined from the momentum balance

$$\sigma_f=\frac{A_{st}}{A}\rho_{bst}U_s^2=\alpha\rho_{bst}U_s^2 \tag{7}$$

where A_{st} is the cross-sectional area of the stationary bed ahead of a slug, α is the cross-sectional area ratio of stationary bed to pipe and ρ_{bst} is the bulk density of solids in the stationary bed, which is approximately equal to the loose-poured bulk density of the solids ρ_b. U_s is the slug velocity (i.e. mean velocity of the particles contained in the slug).

3. Test rig and test materials

It is difficult to predict theoretically the effect of some of the influential parameters, such as slug velocity. Experimental work is required to investigate the influence and relationship of the major parameters. A low-velocity pneumatic conveying test rig is set up to provide long horizontal conveying sections as shown in Fig. 4. The air from a compressor is filtered and cooled before it is introduced into the 105 mm i.d. mild steel conveying line, either 96 or 52 m in length. The flanged connections are installed to provide a continuous and uninterrupted flow area.

The mass flow rate of solids m_s is determined from the load cell readings and the mass flow rate of air m_f is determined by an orifice plate. Static air pressures are measured by pressure transducers. Also, two wall pressure measuring assemblies as shown in Fig. 5 are installed along a horizontal section of the pipe (see Fig. 4). Wall pressure is obtained by subtracting the static air pressure from the total pressure. Slug velocity is determined by calculating the cross-correlation function of the wall pressure signals. Stationary bed thickness is obtained by taking photos of the bed through the sight glass which was connected into the pipeline (see Fig. 4).

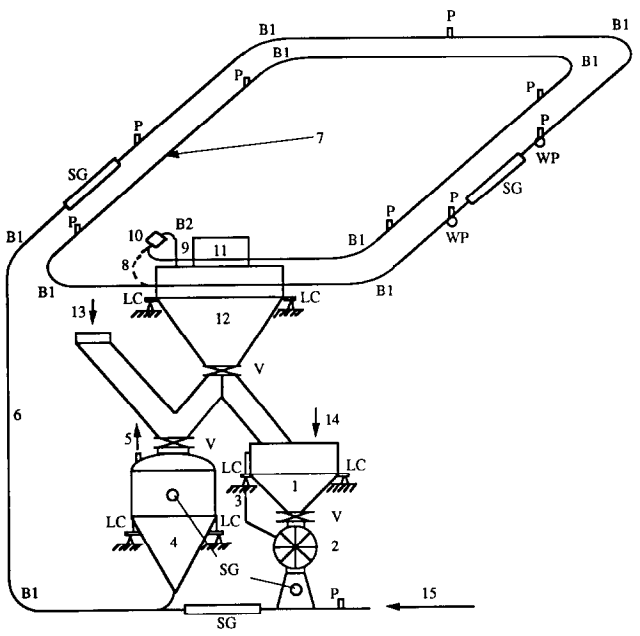

Fig. 4. Schematic layout of low-velocity pneumatic conveying test rig: 1, feed hopper; 2, ZGR-250 rotary valve; 3, air vent pipe; 4, blow tank; 5, blow tank air vent; 6, vertical lift, 6.5 m; 7, transport line 105 mm i.d., one loop 52 m, two loops 96 m; 8, 52 m loop connector; 9, return line; 10, back pressure valve; 11, reverse-jet filter; 12, receiving silo; 13, blow tank filling; 14, rotary valve filling; 15, conveying air inlet; B1, 90° bend 1.0 m Rad; B2, 45° bend; LC, load cells; P, static air pressure tapping; SG, sight glass; V, valves; WP, wall pressure fittings.

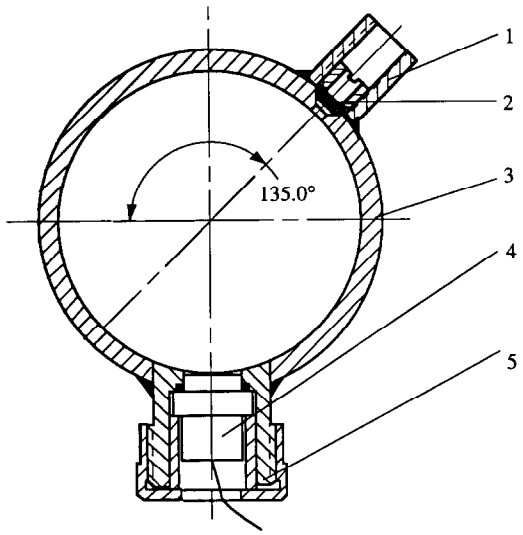

Fig. 5. Wall pressure measuring assembly: 1, static pressure tapping; 2, porous plastic; 3, pipe; 4, AB/HP-50G pressure transducer; 5, AB/HP-50G transducer fitting.

Four types of material are selected for the test program and the main physical properties are listed in Table 1.

4. Experimental results

4.1. Slug velocity

The experimentally determined values of slug velocity U_s are plotted against the corresponding values of superficial air velocity U_a, as shown in Fig. 6. It can be seen that the slug velocity depends strongly on the air velocity for each different test material. For a given product, the data appear to be represented by a linear correlation. It should be noted that each line does not pass through the origin given in Fig. 6. This indicates the minimum air velocity that is needed to initiate the motion of a particle slug in a horizontal pipe. This situation was also described by Legel and Schwedes [3].

Therefore,

$$U_s = k(U_a - U_{a\,min}) \tag{8}$$

where $U_{a\,min}$ is the minimum air velocity for horizontal flow and k is the slope of the line.

It was found [5] that

$$U_{a\,min} = \frac{\rho_s g \tan \phi_w \epsilon^3 d^2}{180(1-\epsilon)\eta} \tag{9}$$

$$k = \epsilon d \left(\frac{\tan \phi_w}{\tan \phi}\right)^{1/3} \times 1000 \tag{10}$$

It should be noted that the empirical Eq. (10) was developed [5] based on tests undertaken on a 105 mm

Table 1
Physical properties of test materials

Bulk solid	d (mm)	ρ_s (kg m^{-3})	ρ_b (kg m^{-3})	γ_b	ϵ	ϕ_w[a] (°)	ϕ (°)
White plastic pellets	3.12	865.1	493.7	0.494	0.430	15.15	44.70
Black plastic pellets	3.76	834.1	458.0	0.458	0.451	12.95	43.76
Wheat	3.47	1449.0	811.5	0.812	0.440	16.01	43.73
Barley	3.91	1350.0	721.7	0.722	0.465	14.20	31.07

[a]Wall material is mild steel.

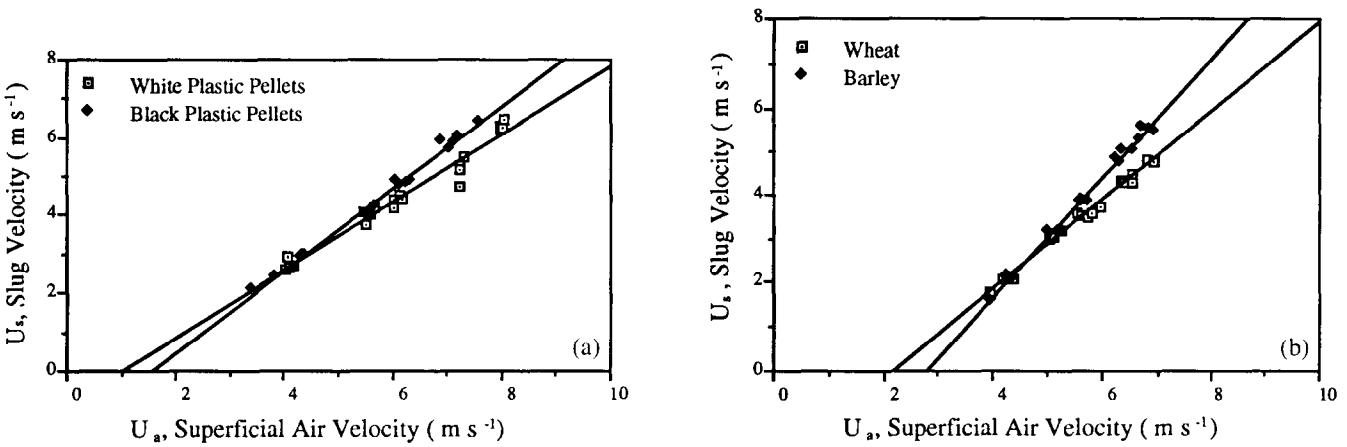

Fig. 6. Slug velocity vs. superficial air velocity for experiments carried out in a 105 mm i.d. mild steel pipeline.

Table 2
Experimental wall pressures and stress transmission coefficients for wheat

No.	52 m pipeline					96 m pipeline				
	m_f	m_s	σ_{rw}	σ_x	λ	m_f	m_s	σ_{rw}	σ_x	λ
1	0.0497	0.967	0.334	0.634	0.527	0.0558	1.159	0.420	0.768	0.547
2	0.0661	0.949	0.671	1.158	0.579	0.0672	1.157	0.702	1.193	0.588
3	0.0733	0.957	0.726	1.346	0.539	0.0747	1.161	0.706	1.310	0.539
4	0.0826	0.953	0.896	1.656	0.541	0.0838	1.168	0.926	1.688	0.601
5	0.0885	0.948	0.978	1.729	0.566	0.0872	1.162	0.969	1.712	0.587
6	0.0495	1.450	0.341	0.622	0.548	0.0560	1.494	0.423	0.762	0.555
7	0.0665	1.439	0.639	1.101	0.580	0.0675	1.494	0.737	1.223	0.603
8	0.0742	1.439	0.785	1.333	0.589	0.0754	1.496	0.796	1.364	0.584
9	0.0835	1.454	0.892	1.604	0.556	0.0832	1.497	0.882	1.529	0.577
10	0.0887	1.464	0.997	1.762	0.566	0.0870	1.493	1.009	1.623	0.622
11	0.0547	1.945	0.442	0.760	0.582	0.0555	1.960	0.423	0.728	0.515
12	0.0675	1.979	0.711	1.234	0.576	0.0675	1.957	0.707	1.191	0.594
13	0.0747	1.982	0.746	1.300	0.573	0.0744	1.968	0.788	1.346	0.585
14	0.0796	1.997	0.814	1.423	0.572	0.0834	1.969	0.948	1.524	0.622
15	0.0868	1.996	0.909	1.597	0.569	0.0877	1.964	1.008	1.703	0.592
16	0.0543	2.300	0.403	0.773	0.521	0.0556	2.387	0.423	0.828	0.511
17	0.0657	2.383	0.663	1.130	0.587	0.0673	2.402	0.673	1.190	0.566
18	0.0749	2.392	0.780	1.364	0.572	0.0746	2.374	0.781	1.357	0.576
19	0.0838	2.389	0.952	1.688	0.564	0.0835	2.373	0.928	1.535	0.605
20	0.0884	2.398	1.028	1.747	0.588	0.0873	2.375	0.996	1.709	0.583

i.d. mild steel horizontal pipeline. Hence, the effect of pipe diameter on the slope k was not able to be taken into account. To investigate the influence of pipe diameter on the slope k, dimensional analysis is employed.

Since k is the slope of a linear model, it should be dimensionless. However, Eq. (10) has a unit of length due to the presence of the particle diameter. By taking the influence of pipe diameter into account (i.e. in-

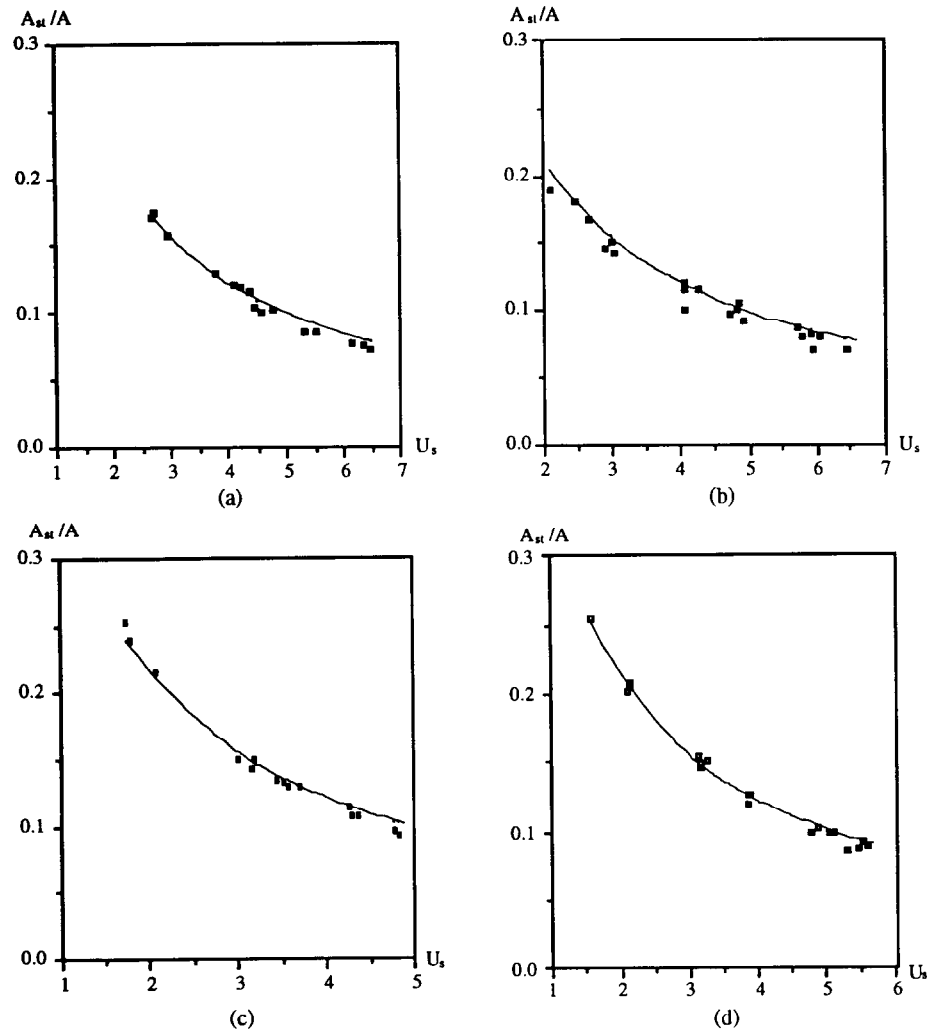

Fig. 7. Cross-sectional area ratio of stationary bed to pipe vs. slug velocity: (a) white plastic pellets; (b) black plastic pellets; (c) wheat; (d) barley.

cluding the pipe diameter in the expression for k), the following dimensionless equation is obtained.

$$k = c_d \frac{\epsilon d}{D} \left(\frac{\tan \phi_w}{\tan \phi} \right)^{1/3} \tag{11}$$

where c_d is a dimensionless coefficient.

The coefficient c_d can be determined by inserting the known slope k, physical properties of the material and pipe diameter into Eq. (11). For example, for white plastic pellets flowing through the 105 i.d. mild steel pipeline in dense-phase:
$k = 0.873$, $\epsilon = 0.430$, $d = 3.12$ mm, $\tan \phi_w = 0.271$, $\tan \phi = 0.990$ and $D = 105$ mm, from which $c_d = 105$ is calculated from Eq. (11).

Hence, for different pipe diameters, the slope k can be determined from

$$k = 105 \frac{\epsilon d}{D} \left(\frac{\tan \phi_w}{\tan \phi} \right)^{1/3} \tag{12}$$

4.2. Stationary bed thickness

The cross-sectional area ratio of stationary bed to pipe can be estimated by Eq. (13) [2]. This equation is plotted in Fig. 7 against the data obtained from the current investigations. The agreement is very good.

$$\alpha = \frac{A_{st}}{A} = \frac{1}{(1 + U_s / 0.542\sqrt{gD})} \tag{13}$$

4.3. Wall pressure and stress transmission coefficient

Table 2 summarises measured wall pressures and corresponding stress transmission coefficients for conveying wheat in dense-phase through 52 and 96 m long pipelines. From the test results listed in Table 2, it can be seen that the values of the stress transmission coefficient are similar with an average value of 0.572 (i.e. despite different conveying conditions and different pipe lengths). The other test results also display similar

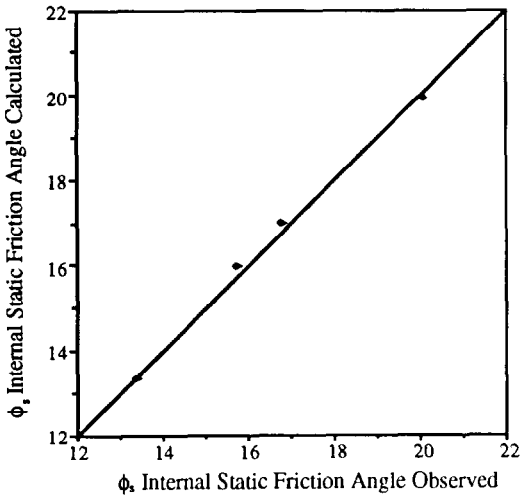

Fig. 8. Internal static friction angle.

trends with average values of $\lambda = 0.756$, 0.806 and 0.655 for white plastic pellets, black plastic pellets and barley, respectively. According to Eqs. (2) and (3), the internal static friction angles are 20.08°, 16.81°, 15.75° and 13.40° corresponding to the average $\lambda = 0.572$, 0.655, 0.756 and 0.806. It should be noted that these experimental results also show that all values of the stress transmission coefficient are less than 1. This indicates that the stress state in slug-flow low-velocity pneumatic conveying should be under active conditions. Using the method of least-squares, the values of ϕ_s are best fitted by the following function:

$$\phi_s = \frac{4}{3}\phi_w \gamma_b^{1/3} \tag{14}$$

where ϕ_w is the wall friction angle and γ_b is the bulk solid specific density with respect to water at 4 °C. The goodness of fit is shown in Fig. 8.

5. Pressure drop in horizontal pipeline

For a single slug of cohesionless material in a horizontal pipe, Eq. (6) is proposed for the prediction of pressure gradient. However, an actual slug-flow pneumatic conveying system usually has several slugs flowing along the pipeline. Since each slug undergoes the same variation in velocity while it flows from the high pressure end to the low pressure end of the pipeline, it is reasonable to assume that every slug flows through the pipeline with the one average velocity. Thus all the moving particles in the pipeline can be treated as one long slug with a length L_s, which represents the sum of the length of all individual slugs, all moving through a pipe of length L_t at a mean slug velocity of U_s. It follows that the mass flow rate of solids, m_s = (mass of moving solids)/(time taken to travel through pipe) and hence

$$L_s = \frac{m_s L_t}{A(1-\alpha)\rho_b U_s} \tag{15}$$

Assuming that the pressure drop caused by the conveying air is small compared with the total pressure drop, l_s in Eq. (6) is replaced with L_s. By substituting Eqs. (7) and (15) into Eq. (6), the pressure drop across the length L_t of a horizontal pipe is found to be

$$\Delta P = (1 + 1.084\lambda \mathrm{Fr}^{0.5} + 0.542\mathrm{Fr}^{-0.5}) \frac{2g\mu_w m_s L_t}{AU_s} \tag{16}$$

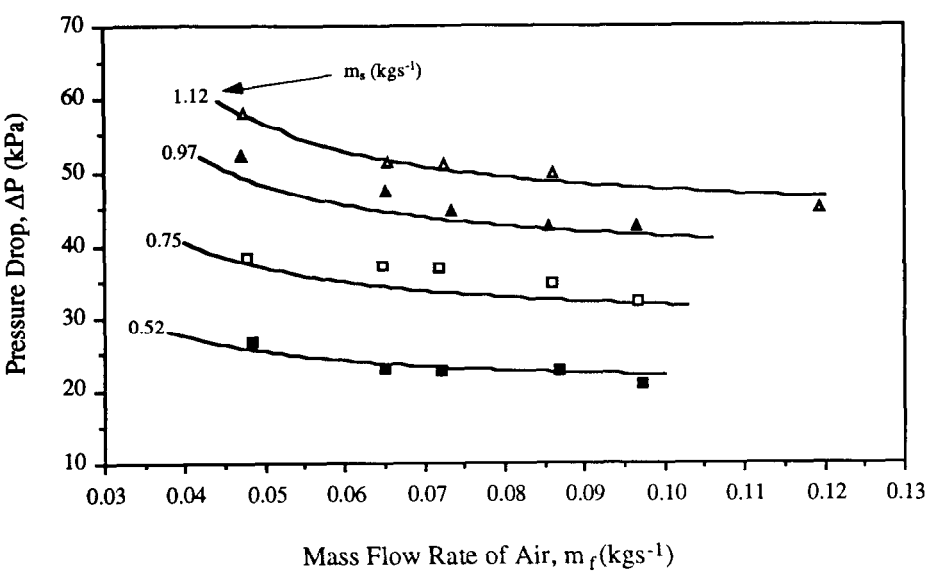

Fig. 9. Predicted conveying characteristics of white plastic pellets for horizontal pipe length $L = 78$ m and $D = 0.105$ m, showing the curves of constant m_s. $m_s = 0.52$ (■), 0.75 (□), 0.97 (▲), 1.12 (△) kg s^{-1}.

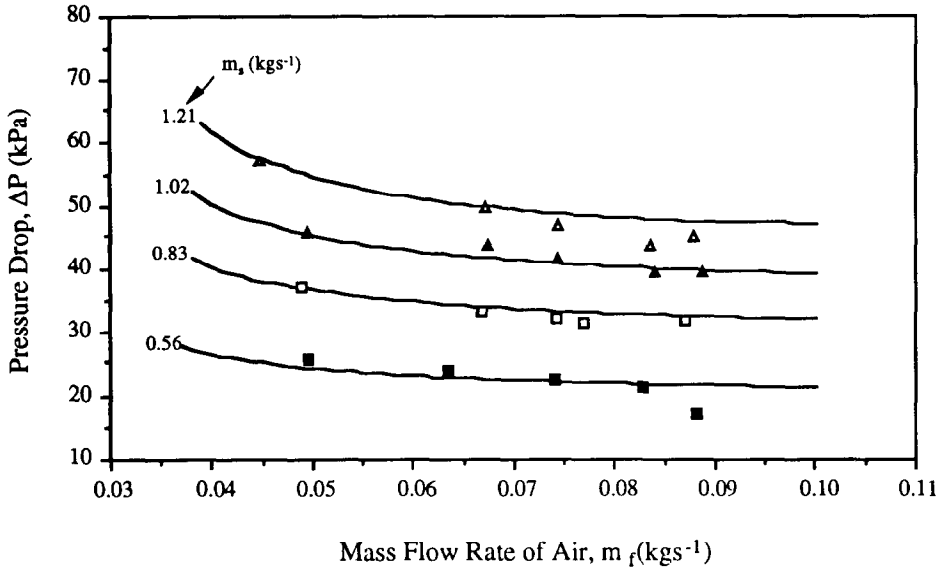

Fig. 10. Predicted conveying characteristics of black plastic pellets for horizontal pipe length $L=78$ m and $D=0.105$ m, showing the curves of constant m_s. $m_s=0.56$ (■), 0.83 (□), 1.02 (▲), 1.21 (△) kg s^{-1}.

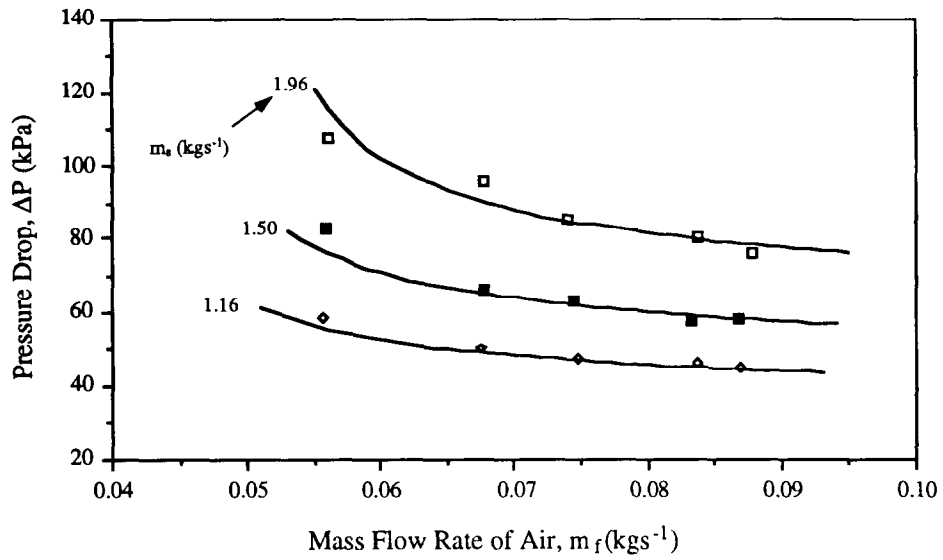

Fig. 11. Predicted conveying characteristics of wheat for horizontal pipe length $L=78$ m and $D=0.105$ m, showing the curves of constant m_s. $m_s=1.16$ (◇), 1.50 (■), 1.96 (□) kg s^{-1}.

where

$$\mathrm{Fr}=\frac{U_s^2}{gD}$$

The mean slug velocity U_s and Froude number Fr in the above equation can be estimated for a given mass flow rate of air m_f, pipe diameter D, and assuming an initial pipeline pressure drop. Therefore, for slug-flow pneumatic conveying and a certain mass flow rate of solids m_s, the pressure drop across a horizontal pipe of length L_t can be predicted using computer iteration. The calculation procedure is listed below.

(i) Calculate the stress transmission coefficient λ, using Eqs. (2), (3) and (14).

(ii) Assume an initial value for the pipeline pressure drop ΔP.

(iii) Calculate the mean air density ρ_a and the mean superficial air velocity U_a.

(iv) Estimate the mean slug velocity U_s from Eq. (8) and determine the Froude number Fr.

(v) Substitute these values of U_s, Fr, and λ into Eq. (16) to calculate the pressure drop.

(vi) Compare with the estimate of pipeline pressure drop in (ii), and repeat from step (iii) onwards until convergence is obtained.

Using the above calculation procedure, curves of constant m_s are predicted for each test material conveyed over various distances, as shown in Figs. 9–12. Such

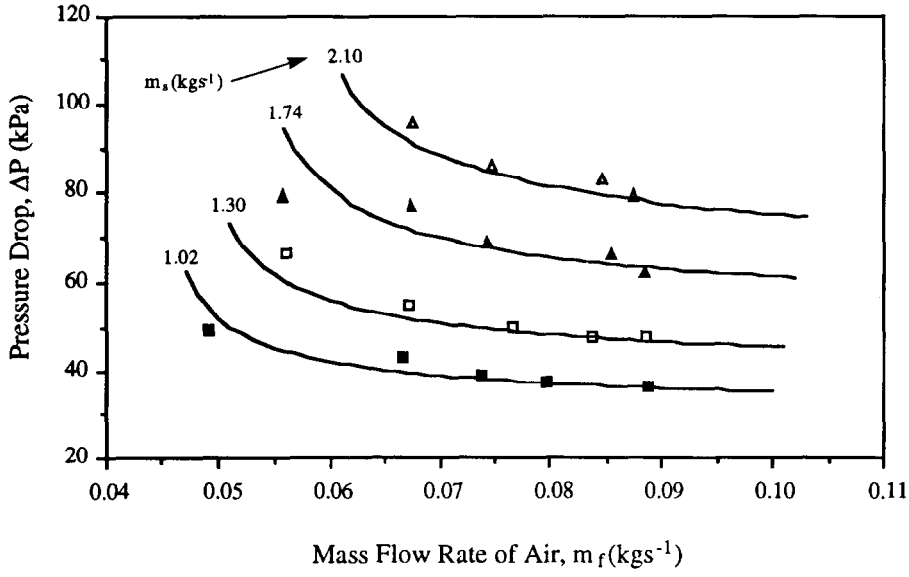

Fig. 12. Predicted conveying characteristics of barley for horizontal pipe length $L=78$ m and $D=0.105$ m, showing the curves of constant m_s. $m_s=1.02$ (■), 1.30 (□), 1.74 (▲), 2.10 (△) kg s^{-1}.

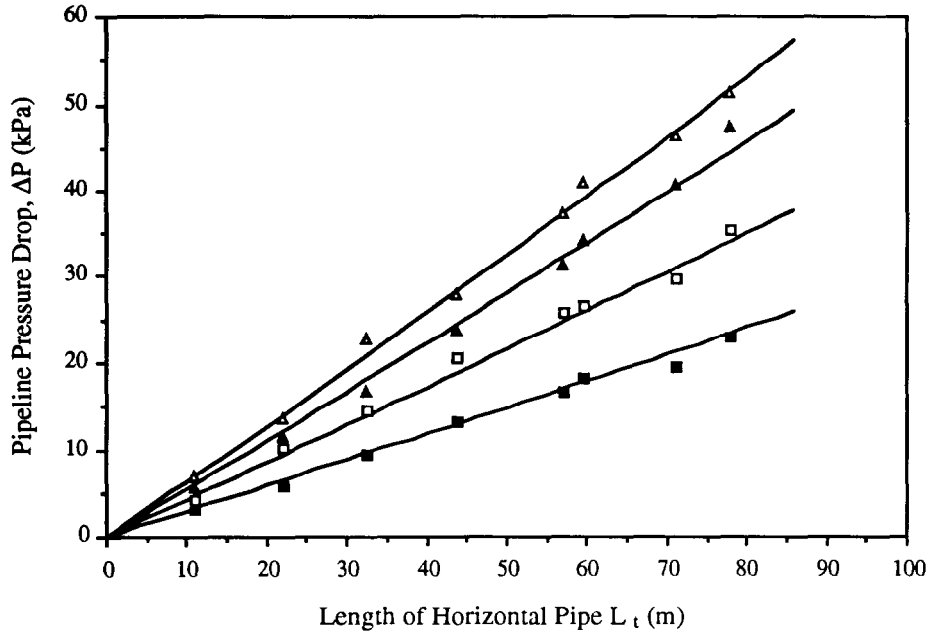

Fig. 13. Predicted pressure distribution for white plastic pellets along a horizontal pipe. ■, $m_f=0.065$; $m_s=0.52$ kg s^{-1}. □, $m_f=0.065$; $m_s=0.75$ kg s^{-1}. ▲, $m_f=0.065$; $m_s=0.96$ kg s^{-1}. △, $m_f=0.066$; $m_s=1.12$ kg s^{-1}.

graphs are referred to as pneumatic conveying characteristics (PCC). The experimental results are superimposed onto each figure for comparison. The pressure distributions along the horizontal pipeline are also calculated from the model for the various test materials, as shown in Figs. 13–16. All these plots show good agreement between the predicted curves and experimental data.

To investigate further the applicability and scale-up accuracy of the above method, an additional test program was carried out on polystyrene chips. Table 3 lists the experimental results obtained on three different test rigs. Test rig 1 is the 96 m low-velocity pneumatic conveying test rig shown in Fig. 4. Test rigs 2 and 3 both use a 156 mm i.d. mild steel pipeline, 52 m in length. Note that the pipe layout is similar to the 52 m pipeline shown in Fig. 4. Test rig 3 uses a ZGR-250 rotary valve feeder, whereas test rig 2 uses a 0.9 m^3 blow tank. The reason for employing different feeders is to establish their effect on the conveying performance of polystyrene chips. The use of different material feeders was found to have little influence on the material's *pipeline* pneumatic conveying characteristics. The predicted values of pressure drop ΔP_c are listed in the

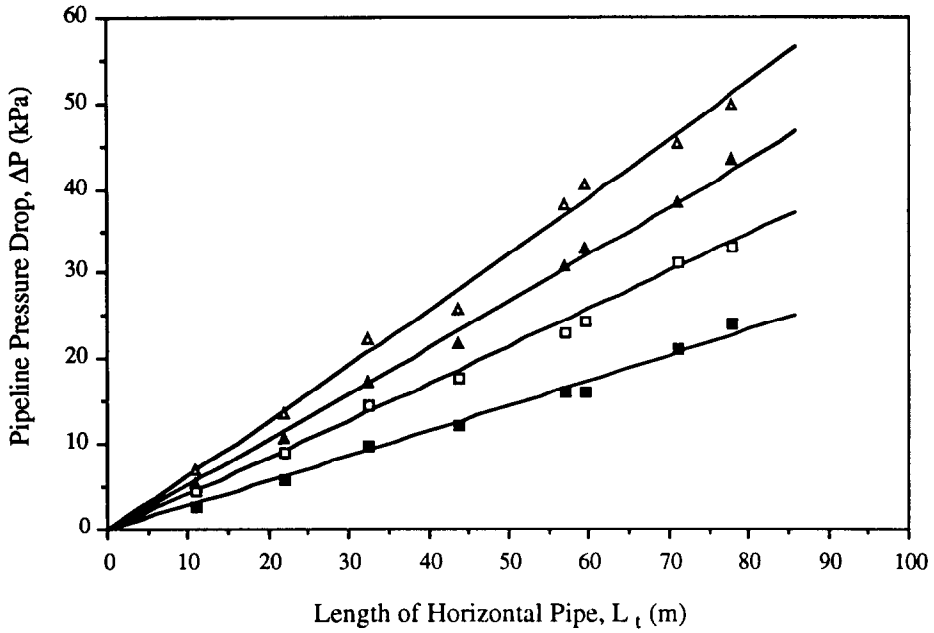

Fig. 14. Predicted pressure distribution for black plastic pellets along a horizontal pipe. ■, $m_f = 0.064$; $m_s = 0.56$ kg s^{-1}. □, $m_f = 0.067$; $m_s = 0.83$ kg s^{-1}. ▲, $m_f = 0.068$; $m_s = 1.03$ kg s^{-1}. △, $m_f = 0.067$; $m_s = 1.24$ kg s^{-1}.

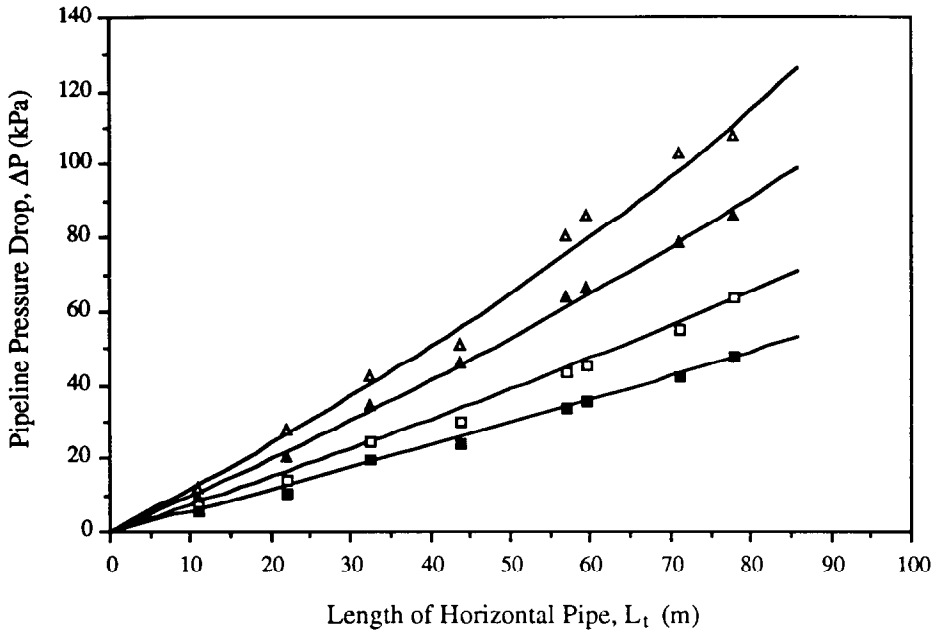

Fig. 15. Predicted pressure distribution for wheat along a horizontal pipe. ■, $m_f = 0.075$; $m_s = 1.16$ kg s^{-1}. □, $m_f = 0.074$; $m_s = 1.50$ kg s^{-1}. ▲, $m_f = 0.074$; $m_s = 1.97$ kg s^{-1}. △, $m_f = 0.074$; $m_s = 2.37$ kg s^{-1}.

last column of Table 3 and compare well with the experimental values ΔP_e. A graphical comparison is also shown in Fig. 17.

6. Minimising power in slug-flow pneumatic conveying

The low-velocity slug-flow pneumatic conveying characteristic curves shown in Figs. 9–12 show that for a given m_s, ΔP decreases with increasing m_f. Also, it can be seen that the pressure gradient increases quite sharply at low values of m_f. Theoretically, it is possible to operate at any point along the m_s curve. However, from an energy point of view, this may not be feasible. That is, it is desirable to operate the slug-flow system at minimal energy. The following equation can be used to calculate the nominal power required for conveying.

$$N_n = \Delta P A U_a \tag{17}$$

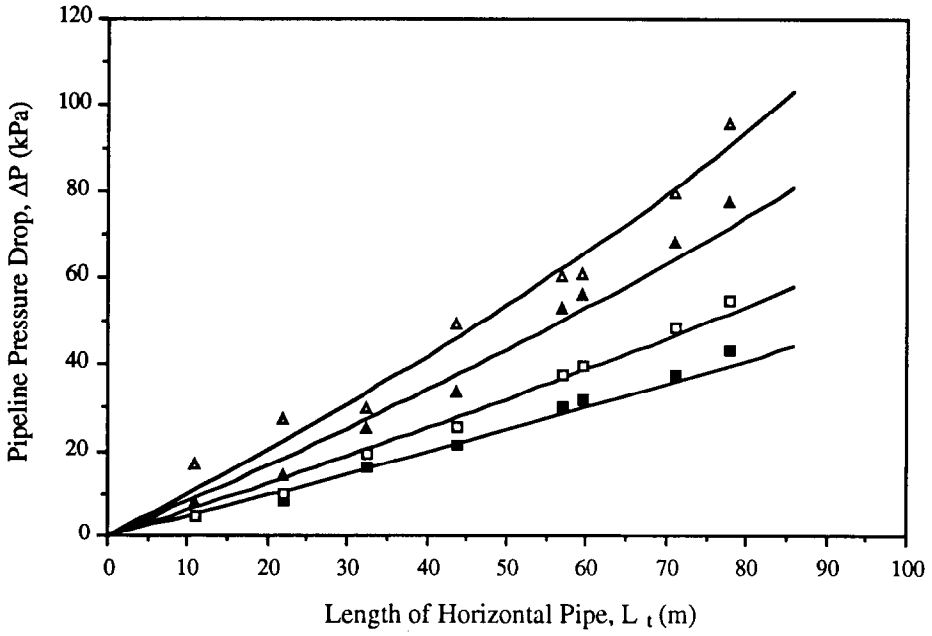

Fig. 16. Predicted pressure distribution for barley along a horizontal pipe. ■, m_f=0.067; m_s=1.00 kg s^{-1}. □, m_f=0.067; m_s=1.29 kg s^{-1}. ▲, m_f=0.068; m_s=1.73 kg s^{-1}. △, m_f=0.068; m_s=2.11 kg s^{-1}.

Table 3
Steady-state dense-phase results for clear polystyrene chips

Test rig	Exp. No.	Speed[a] (rpm)	m_{ft} (kg s^{-1})	m_{ft} (kg s^{-1})	m_f (kg s^{-1})	m_s (kg s^{-1})	ΔP_e (kPa)	ΔP_c (kPa)
1	4	20	0.083	0.027	0.056	1.279	71.0	72.15
	5	30	0.084	0.036	0.048	1.714	111.0	115.35
	6	42	0.084	0.037	0.047	1.804	126.0	127.09
	7	35	0.085	0.037	0.048	1.764	118.0	118.51
	10	35	0.083	0.038	0.045	1.782	121.0	128.05
	11	35	0.104	0.034	0.070	1.900	102.0	100.75
	15	27	0.084	0.033	0.051	1.570	104.0	97.67
	19	18	0.084	0.024	0.060	1.150	68.0	61.38
	21	18	0.073	0.027	0.045	1.182	78.0	76.56
2	57		0.193		0.193	8.57	107.0	104.76
	58		0.181		0.181	8.82	109.0	114.32
	59		0.187		0.187	8.28	101.0	102.74
	60		0.141		0.141	6.49	91.0	96.16
	64		0.142		0.142	6.87	105.0	103.03
	65		0.141		0.141	7.04	102.0	107.33
	66		0.099		0.099	4.67	87.0	94.27
3	102	35	0.090	0.019	0.071	1.95	41.5	44.89
	103	35	0.109	0.018	0.091	2.00	37.8	37.61
	104	35	0.108	0.017	0.091	2.00	37.0	37.61
	105	35	0.128	0.015	0.128	2.10	33.4	31.65
	106	35	0.150	0.013	0.137	2.10	28.0	27.07
	110	21	0.080	0.016	0.064	1.43	34.0	36.22
	111	21	0.097	0.013	0.084	1.43	26.0	25.93
	112	21	0.118	0.012	0.106	1.45	22.3	23.24
	113	21	0.135	0.011	0.124	1.47	22.4	20.45

[a]Rotary valve speed.

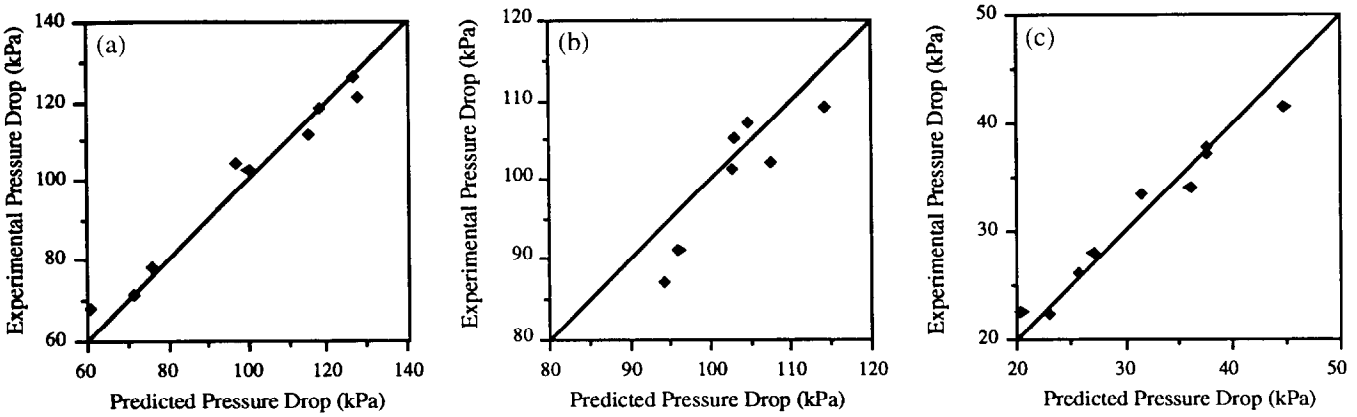

Fig. 17. Predicted pressure drop compared with experimental pressure drop obtained on (a) test rig 1, (b) test rig 2 and (c) test rig 3 for clear polystyrene chips with physical properties: $d=2.98$ mm, $\rho_b=637.0$ kg m^{-3}, $\epsilon=0.387$, $\phi=44.6°$, $\phi_w=15.8°$.

Table 4
Economical superficial air velocity and mass flow rate of air

Test material	U_a (m s^{-1})	m_s (kg s^{-1})	36 m Horizontal pipe		78 m Horizontal pipe	
			m_f (kg s^{-1})	ΔP (kPa)	m_f (kg s^{-1})	ΔP (kPa)
White plastic pellets	2.762	0.52	0.032	18.55	0.035	40.37
		0.76	0.033	27.33	0.037	60.44
		1.00	0.034	36.26	0.040	78.66
		1.16	0.035	41.81	0.042	90.60
Black platic pellets	3.071	0.56	0.035	16.56	0.038	35.97
		0.84	0.036	25.08	0.041	53.75
		1.04	0.037	31.00	0.043	66.65
		1.22	0.038	36.20	0.045	77.83
Wheat	4.738	1.06	0.056	27.31	0.064	59.15
		1.47	0.059	37.85	0.070	82.03
		1.97	0.062	50.78	0.076	110.00
		2.38	0.064	61.33	0.082	132.90
Barley	5.102	1.03	0.059	23.24	0.067	50.36
		1.31	0.061	29.56	0.070	64.06
		1.74	0.064	39.15	0.076	84.85
		2.11	0.066	47.50	0.080	102.90

Substituting Eq. (17) into Eq. (16), and making N_n the subject results in

$$N_n=(1+1.084\lambda \mathrm{Fr}^{0.5}+0.542\mathrm{Fr}^{-0.5})\frac{2g\mu_w m_s L_t}{U_s}U_a \quad (18)$$

To minimise power consumption, Eq. (18) is differentiated with respect to U_a and allowed to be equal to zero. That is,

$$k^2U_a^3-3k^2U_{a\,min}U_a^2+\left(3k^2U_{a\,min}^2-\frac{\sqrt{gD}}{1.084\lambda}kU_{a\,min}-\frac{gD}{2\lambda}\right)U_a-\left(k^2U_{a\,min}^3-\frac{\sqrt{gD}}{1.084\lambda}kU_{a\,min}^2+\frac{gD}{2\lambda}U_{a\,min}\right)=0 \quad (19)$$

Three roots of solution can be obtained from Eq. (19). Actual calculations have found that two of them are complex and obviously unrepresentative of a real system. The real root is the mean superficial air velocity which minimises energy consumption. From Eq. (19), it can be seen that this 'economical' superficial air velocity is representative of a given conveyed material and pipe diameter. However, the corresponding 'economical' value of m_f is still dependent on the mass flowrate of solids and pipe length (i.e. due to the air flow being compressible).

'Economical' superficial air velocities and mass flowrates of air for different solids mass flowrates and pipe lengths are calculated from Eq. (19) for black plastic pellets, white plastic pellets, wheat and barley conveyed through a 105 mm i.e. horizontal pipeline. The results are given in Table 4 and demonstrate the dependency of 'economical' m_f on m_s and L.

7. Conclusions

1. A theoretical expression for the pressure gradient of horizontal slug-flow is developed by applying the principles of powder mechanics to a moving slug. This expression indicates that the air pressure balances the resistance forces due to the material weight of the slug and the transmission radial stress caused by the interaction of particles.

2. The transmission radial stress depends mainly on the stress transmission coefficient and the slug velocity, which appears to be independent of the mass flowrate of solids, but varies linearly with the superficial air velocity.

3. The solid particles in the slug travel basically at the same velocity and are fixed relative to each other except in the vicinity of the front and back faces of the slug. Hence, failure occurs only at the boundary between the pipe wall and slug (i.e. instead of inside the slug).

4. The interparticle stresses in a horizontal moving slug appear to be in the active state. Combined with failure theory, a semi-empirical expression of the stress transmission coefficient has been developed.

5. Based on the theoretical expression of pressure gradient for moving slugs and the experimental results of slug velocity and stress transmission coefficient, a semi-empirical model has been developed for predicting total horizontal pipeline pressure drop. Predicted values of pressure drop and pressure distribution along various pipelines compare well with the experimental data.

6. 'Economical' superficial conveying air velocity can be determined by a third-order equation which is generated on the basis of minimum energy consumption. The solution is a fixed value for a given material and pipe diameter and is not affected by the mass flow rate of conveyed solids and pipe length.

8. List of symbols

A	cross-sectional area of pipe (m^2)
A_{st}	cross-sectional area of stationary bed (m^2)
c_d	dimensionless coefficient
c_w	particle cohesion at wall
d	particle diameter (m)
D	inner pipe diameter (m)
Fr	Froude number
g	acceleration due to gravity (m s^{-2})
k	slope of line defined in Eq. (8)
l_s	length of single slug (m)
L_s	total length of slugs (m)
L_t	total horizontal pipeline length (m)
m	mass of particles (kg)
m_f	actual mass flowrate of air through pneumatic conveying pipeline (kg s^{-1})
m_{fl}	rotary valve air leakage (kg s^{-1})
m_{ft}	total supplied mass flowrate of air (kg s^{-1})
m_s	mass flow rate of solids (kg s^{-1})
N_n	nominal power (W)
p	interstitial air pressure (Pa g)
Δp	pressure drop across a single horizontal slug (Pa)
P_s	stress in Fig. A-1 (Pa)
ΔP	total horizontal pipeline pressure drop (Pa)
ΔP_c	predicted value of total horizontal pipeline pressure drop (Pa)
ΔP_e	experimental value of total horizontal pipeline pressure drop (Pa)
r	radius of Mohr circle
R	inner pipe radius (m)
U_a	superficial air velocity (m s^{-1})
$U_{a\ min}$	minimum superficial air velocity (m s^{-1})
U_{pst}	particle velocity in stationary bed (m s^{-1})
U_s	slug velocity (m s^{-1})
U_{sf}	velocity of front or back face of slug (m s^{-1})
x	horizontal coordinate

Greek letters

α	cross-sectional area ratio of stationary bed to pipe
ϵ	bulk voidage
ϕ	internal friction angle (°)
ϕ_s	static internal friction angle (°)
ϕ_w	wall friction angle (°)
γ_b	bulk specific gravity with respect to water at 4 °C
λ	stress transmission coefficient
μ_w	wall friction coefficient
ρ	density of a liquid (kg m^{-3})
ρ_a	air density (kg m^{-3})
ρ_b	bulk density (kg m^{-3})
ρ_{bst}	bulk density of stationary bed (kg m^{-3})
ρ_s	particle density (kg m^{-3})
σ_b	normal stress at the back face of slug (Pa)
σ_f	normal stress at the front face of slug (Pa)
σ_n, τ_n	coordinate
σ_r	radial stress of particle slug (Pa)
σ_{sw}	normal wall stress due to material weight (Pa)
σ_{rw}	radial stress of a particle slug at wall (Pa)
σ_w	wall pressure, i.e. total normal wall stress (Pa)
σ_x	axial stress of particle slug (Pa)
τ_w	shear stress at wall (Pa)

Appendix

It has been determined [4] that the Mohr circle, which represents the stress of an element in a particle slug, should be located between the wall yield locus and the material's yield locus, as shown in Fig. A-1. Line OF tangent to the Mohr circle passes through the origin of the σ_n–τ_n coordinate system. The angle between the line OF and σ_n axis is defined as static internal friction angle. The stress transmission coefficient under active conditions can be determined by trigonometry, as follows.

Applying the sine rule to triangle OAC in Fig. A-1

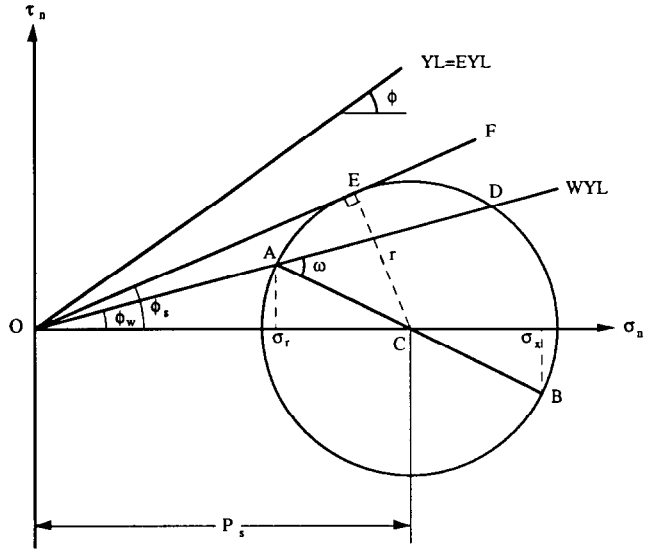

Fig. A-1. Mohr circle representation of stress in particle slug.

$$\sigma_r = P_s - r\cos(\omega - \phi_w) \tag{A-1}$$

$$\sigma_x = P_s + r\cos(\omega - \phi_w) \tag{A-2}$$

$$\frac{P_s}{\sin(\pi - \omega)} = \frac{r}{\sin\phi_w} \tag{A-3}$$

From triangle OEC

$$P_s = \frac{r}{\sin\phi_s} \tag{A-4}$$

Substituting Eq. (A-4) into Eqs. (A-1) and (A-2) and eliminating r

$$\lambda_A = \frac{\sigma_r}{\sigma_x} = \frac{1 - \sin\phi_s\cos(\omega - \phi_w)}{1 + \sin\phi_s\cos(\omega - \phi_w)} \tag{A-5}$$

Also, substituting Eq. (A-4) into Eq. (A-3) and eliminating r

$$\sin\omega = \sin\phi_w / \sin\phi_s \tag{A-6}$$

References

[1] P.W. Wypych and G. Hauser, *Proc. Pneumatech 4, Int. Conf. Pneumatic Conveying Technology, Glasgow, Scotland, 1990,* Powder Advisory Centre, UK, pp. 241–260.

[2] K. Konrad and D. Harrison, *Proc. Pneumotransport 5, Fifth Int. Conf. Pneumatic Transport of Solids in Pipes, London, UK, 1980,* BHRA Fluid Engineering, pp. 225–244.

[3] D. Legel and J. Schwedes, *Bulk Solids Handling, 4* (1984) 399–405.

[4] B. Mi and P.W. Wypych, *Int. Res. Rep. 93-05-BM-1,* Department of Mechanical Engineering, University of Wollongong, NSW, Australia, May, 1993.

[5] B. Mi and P.W. Wypych, *Powder Handling Process., 5* (3) (1993) 227–233.